Design of photonic directional couplers as phase selectors

Po-Yi Lee, Chih-Hsien Huang, and Wen-Feng Hsieh*

Department of Photonic & Institute of Electro-Optical Engineering, National Chiao Tung University, Hsinchu 300, Taiwan
**Corresponding author: wfhsieh@mail.nctu.edu.tw*

Received February 19, 2013; revised April 20, 2013; accepted April 20, 2013; posted April 22, 2013 (Doc. ID 185467); published May 22, 2013

A phase selector is designed by relatively sliding two coupled identical photonic crystal waveguides (PCWs) of a photonic directional coupler (DC). By solving the coupled equations analytically derived from the tight-binding theory, symmetry breaking in the crossing of dispersion curves can be observed as countersliding two degenerated waveguides along the propagation direction. There exists a different phase shift between two eigenmodes by varying the sliding distance and the operating frequency. Numerical simulations of DCs made of photonic crystal slabs were used to verify the correctness of our theoretical predictions and to discuss thoroughly the underlying physics of the symmetry-breaking system. The design concept is provided for a phase selector or a beam splitter whose output phase difference can be controlled by the sliding distance of two PCWs. © 2013 Optical Society of America

OCIS codes: (060.1810) Buffers, couplers, routers, switches, and multiplexers; (130.2790) Guided waves; (230.5298) Photonic crystals; (230.7400) Waveguides, slab.
http://dx.doi.org/10.1364/JOSAB.30.001631

1. INTRODUCTION

Photonic crystals (PCs) are the structures in which the dielectric media are arranged periodically and attract a great deal of attention in fabricating photonic integrated devices [1–9]. One of these promising devices, the photonic crystal waveguide (PCW), is created by inserting a row of defects into a PC that allows the light wave to propagate with low loss even through a sharp bend [10]. The directional coupler (DC), which is made of a pair of parallel PCWs separated by one or several rows of partition rods or holes, can be applied to optical switches [11–14], beam splitters [1,15], and modulators [16].

In a symmetrical DC made of two coupled identical waveguides, an electromagnetic (EM) wave with a given frequency incident into one waveguide of the DC will transfer entirely to the other waveguide after a certain distance, called the coupling length and defined as $\pi/\Delta k$ [17]. Here Δk is the wavevector mismatch of the even and odd modes of the DC at the operating frequency. In conventional DCs made of two coupled dielectric waveguides, the coupling between these two identical waveguides removes the degeneracy or breaks the symmetry to cause splitting or anticrossing of dispersion curves [18]. However, in a symmetrical DC made of two identical PCWs, the waveguides are composed of periodic distributed defect rods or holes, so the coupling coefficients are periodic functions of propagation distance. The propagation-dependent coupling between two PCWs can be expanded into two terms under tight-binding approximation [18]. The first term involving the coupling between the nearest-neighbor defects of the two PCWs causes constant splitting of the two dispersion curves, while the second term involving the coupling between the second nearest-neighbor defects sinusoidally modulates the split dispersion curves. Thus, the degeneracy of the two dispersion curves may be removed at all frequencies but leaves a certain frequency where the two dispersion curves cross [18]. At this crossing point with an infinite coupling length or called the decoupling point, no energy transfers between PCWs. The mode parities of the DCs also switch when varying the mode frequency across this decoupling point.

When designing wavelength-selective devices such as demultiplexers [19], manipulating the crossing point and the dispersion relation of a DC is a remarkable issue in getting the proper coupling length in the range of operating frequency for optical communication. There are several ways to approach this manipulation. Here we suggest two methods to control the coupling length through removing the crossing point. One is by way of reducing the coupling between the second nearest-neighbor defects of the two PCWs or increasing the coupling between the nearest-neighbor defects, which can be achieved by sliding the two PCWs in the DC. As the modulating frequency caused by the coupling of the second nearest-neighbor defects is smaller than the splitting frequency of two dispersion curves caused by coupling of the nearest-neighbor defects, the dispersion curves will not cross and the degeneracy or symmetry at the crossing point will be removed. The other way is to use an asymmetrical DC, which contains two PCWs made of different defects. For an asymmetrical DC, for example, with different radii or refractive indices of defects in the two PCWs [17], the dispersion curves can only degenerate into the frequencies of the two nonidentical single PCWs at decoupling or degenerated points, but the eigenfrequencies of two single PCWs are different at this decoupling point. Therefore, the dispersion curves do not cross.

This aim of breaking symmetry of the degenerate DC made of identical PCWs can also be achieved through introducing the optical Kerr media to one PCW of the DC such that the optical Kerr effect causes the difference of the refractive index of the two PCWs. This symmetry breaking through nonlinear modulation of refractive indices of PCWs can be carried out by, for example, embedding the quantum dots in the defect structure of one PCW [6]. However, in such an asymmetric DC, the energy in one PCW cannot completely transfer into the other waveguide due to different electric field ratio of the eigenmodes between two PCWs [17]. Therefore, it is not so practical to make a DC in which the complete energy transfer is requested.

Another symmetry breaking is observed as countersliding two identical PCWs with the same distances along the propagation direction. These two PCWs in this type of longitudinally countersliding DC (LCS-DC) are degenerate; i.e., the dispersion relations of individual waveguides are identical, but symmetry breaking can still be observed in these LCS-DCs. To our knowledge, this phenomenon has never been reported and no theoretical explanation of this type of symmetry breaking exists that leads to anticrossing of the dispersion. Therefore, a theoretical and numerical study of this phenomenon in such a practical device is quite necessary due to not only its academic interest but also its physical concepts for designing the optical devices.

In this paper, we first introduce the general tight-binding theory (TBT) to derive an analytical solution to describe such a symmetry-breaking DC. Second, wave-guiding properties of such a DC are discussed. Third, a practical DC made of a photonic crystal slab (PCS) with air holes is studied numerically using the plane wave expansion method (PWEM) [20] to verify the correctness of our theory through sliding two PCWs of the DC. Finally, the applications of the symmetry-breaking DCs and derived coupled equations are given.

2. TIGHT-BINDING THEORY

We consider a PCW made of a PCS with lattice constant a. The radius of air holes or dielectric rods in the PCW is either enlarged or reduced to support a single propagation mode as shown in Fig. 1(a). To generalize the discussion in the PCS-DC, we consider that all of the defects in each PCW can be slid with respect to the perfect PC shown in Fig. 1(b) so that the distance of the next-neighbor defects between two PCWs can be varied. Here, we only consider the same shift distance of the air holes along the x and y axis at the same (or opposite) direction for mutual-sliding (or countersliding) DCs, as shown in Fig. 2. When the sliding distances are not the same, the DC becomes asymmetrical. The results can be obtained by a similar method, but this is far from the scope of this paper.

Under the TBT, the electric field in the PCWs can be written as the superposition of the electric field $\mathbf{E}_0(\mathbf{r})$ of point defects at different sites. Therefore, the time evolution of the field amplitude (u_n^i) at the nth site of the ith PCW or PCW$_i$ with $i = 1$ and 2 involves coupling between the electric fields of the neighbor sites [21],

$$i\frac{\partial}{\partial t}u_n^i = (\omega_0 - C_0^{ii})u_n^i - \sum_{j=1}^{2}\sum_{m=1}^{3} C_m^{ij}(u_{n+m}^j + u_{n-m}^j). \quad (1)$$

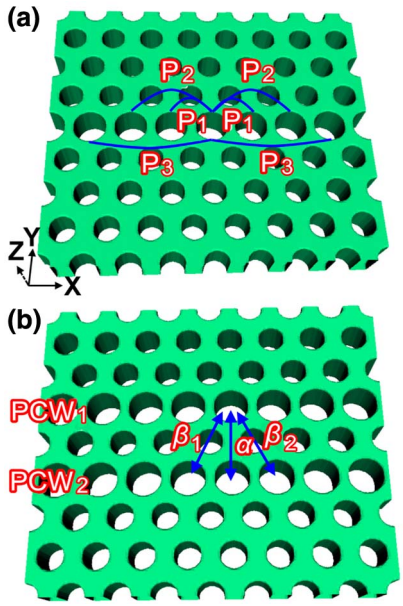

Fig. 1. Geometric structures of (a) single and (b) double PCWs with the lattice constant a. P_m's are the coupling coefficients between defects within a single waveguide. α, β_1, and β_2 are the coupling coefficients between two PCWs.

Here, ω_0 is the eigenfrequency of a point defect, C_0^{ii} represents a small shift in frequency due to the perturbation of the dielectric constant in both PCWs on the site n, and C_m^{ij} represents the coupling coefficients between the site n of PCW$_i$ and the site $n+m$ of PCW$_j$, defined as

$$C_m^{ij} = \frac{\omega i \int_{-\infty}^{\infty} d\nu \Delta\varepsilon(r)\mathbf{E}_{i,n}^* \cdot \mathbf{E}_{j,n+m}}{\int_{-\infty}^{\infty} d\nu[\mu_0|\mathbf{H}_{i,n}|^2 + \varepsilon|\mathbf{E}_{i,n}|^2]}. \quad (2)$$

Here $\mathbf{E}_{i,n}$ and $\mathbf{E}_{j,n+m}$ indicate electric fields of the site n in PCW$_i$ and the site $n+m$ in PCW$_j$, respectively, and $\Delta\varepsilon(r)$ is the difference between the perturbed and the unperturbed dielectric constants.

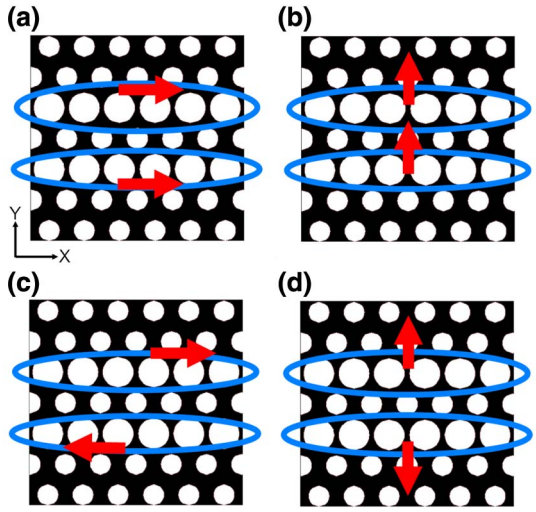

Fig. 2. Types of sliding coupled waveguides: (a) mutual-sliding along x axis, (b) mutual-sliding along y axis, (c) countersliding along x axis, and (d) countersliding along y axis.

In a single PCW, the dispersion relation of the single PCW can be derived as

$$\omega_1(k) = \omega_0 - P_0 - \sum_{m=1}^{3} 2P_m \cos(mka), \tag{3}$$

in which $P_0 = C_0^{ii}$ causes the relative frequency shift for all the wavevector $k's$ from the single defect frequency ω_0 and $P_m = C_m^{ii}$ causes the sinusoidal modulation. The time evolution equations of field amplitudes in two PCWs of a DC are shown as the following when the coupling coefficients α and $\beta_{1,2}$ between two PCWs are considered:

$$i\frac{\partial}{\partial t}u_n^1 = (\omega_0 - C_0^{11})u_n^1 - \sum_{m=1}^{3} C_m^{1j}(u_{n+m}^j + u_{n-m}^j) - \alpha u_n^2 - \beta_1 u_{n-1}^2 - \beta_2 u_{n+1}^2, \tag{4}$$

$$i\frac{\partial}{\partial t}u_n^2 = (\omega_0 - C_0^{22})u_n^2 - \sum_{m=1}^{3} C_m^{2j}(u_{n+m}^j + u_{n-m}^j) - \alpha u_n^1 - \beta_1 u_{n+1}^1 - \beta_2 u_{n-1}^1. \tag{5}$$

Here $\alpha = C_0^{12} = C_0^{21}$, $\beta_1 = C_{-1}^{12} = C_{+1}^{21}$ and $\beta_2 = C_{+1}^{12} = C_{-1}^{21}$ are the coupling coefficients between two PCWs induced by the nearest-neighbor and the next nearest-neighbor defects of one PCW onto the other PCW. Assuming the time-varying field amplitudes have the forms $u_n^1(t) = U_0 \exp(ikna - i\omega t)$ and $u_n^2(t) = V_0 \exp(ikna - i\omega t)$, substituting them into Eqs. (4) and (5), we obtain the characteristic equations of the DC as

$$(\omega - \omega_1')U_0 + (\alpha + 2\beta_1 \cos(ka) + (\beta_2 - \beta_1)\exp(ika))V_0 = 0; \tag{6}$$

$$(\omega - \omega_1')V_0 + (\alpha + 2\beta_1 \cos(ka) + (\beta_2 - \beta_1)\exp(-ika))U_0 = 0. \tag{7}$$

Here U_0 and V_0 are the field amplitudes of PCW_1 and PCW_2, ω is the eigenfrequency of the DC, and $\omega_1'(k) = \omega_1(k) + \Delta\omega_1(k)$ is the eigenfrequency of a single PCW with the additional term $\Delta\omega_1(k)$ in the presence of the other PCW. Generally, the perturbation $\Delta\omega_1$ is small and only causes a slight shift in the dispersion curves. Therefore, the dispersion curves of this DC derived from Eqs. (6) and (7) are

$$\omega(k)^{\pm} = \omega_1(k) + \Delta\omega_1(k) \pm \{g(k)^2 + [\Delta\beta \sin(ka)]^2\}^{1/2} \tag{8}$$

with $g(k) = \alpha + (\beta_1 + \beta_2)\cos(ka)$ and $\Delta\beta = \beta_1 - \beta_2$.

From Eq. (8), two dispersion curves of the DC are split from the single PCW ones that will cross only at $k = 0$ or π/a when $(\beta_2 + \beta_1)/\alpha = -1$ or $+1$ if $\Delta\beta \neq 0$. This criterion is difficult to be reached because in general the signs of the coupling coefficients α and $\beta_{1,2}$ are all negative [22]. Therefore, the dispersion curves will not cross if the next nearest-neighbor coupling coefficients ($\beta_{1,2}$) are not equal. Substitute Eq. (8) into Eqs. (6) and (7); one has the amplitude ratio of PCW_1 and PCW_2 for two eigenmodes,

$$\left(\frac{V_0}{U_0}\right)^{\pm} = \mp\frac{g(k) + i\Delta\beta \sin(ka)}{\sqrt{[g(k)]^2 + \Delta\beta^2 \sin^2(ka)}} = \begin{cases} \mp e^{i\phi}, & g(k) > 0 \\ \pm e^{i\phi} & g(k) < 0 \end{cases} \tag{9}$$

with

$$\phi = \tan^{-1}[\Delta\beta \sin(ka)/g(k)]. \tag{10}$$

Here the "+" sign stands for the high-frequency eigenmode, while the "−" sign stands for the low-frequency one. There exists a phase difference ϕ between the amplitudes of two PCWs for an eigenmode if $\Delta\beta \neq 0$. The phase difference depends upon the propagation wavevector or frequency. The energy incident from one PCW can completely couple into the other waveguide because $|U_0/V_0| = 1$.

As $\beta_1 = \beta_2 = \beta$, Eq. (8) reduces to

$$\omega(k) = \omega_1(k) + \Delta\omega_1(k) \pm (\alpha + 2\beta \cos(ka)), \tag{11}$$

and the phase difference ϕ is either 0 or π at any frequency for the symmetric DC. In this case, two dispersion curves will cross and the mode parities will switch at $k = [\cos^{-1}(-\alpha/2\beta)]/a$ when $|2\beta/\alpha| > 1$. The crossing wavevector decreases as $|2\beta/\alpha|$ increases. Mutually sliding the two PCWs along the x and y directions, or countersliding along the y direction is suitable for Eq. (11) since β_1 always equals β_2 during the slide. On the other hand, when these two PCWs are counter slid along the x direction, β_1 is not equal to β_2 and Eqs. (8) and (10) should be used to describe the dispersion relation and the phase difference of the two PCWs. The existence of mismatch between the second nearest-neighbor coupling coefficients, $\Delta\beta \neq 0$, causes symmetry breaking. The dispersion curves do not cross even with a small slide, and the phase difference ϕ between the amplitudes of the two PCWs for an eigenmode depends upon the sliding distance and the operation frequency.

3. SIMULATION RESULTS IN PHOTONIC CRYSTAL SLAB AND APPLICATIONS

To study the propagation properties caused by sliding the two PCWs in a DC, we consider a PCS in a triangular lattice with lattice constant a made of a silicon-on-insulator (SOI) substrate [23]; the radius of the air holes, and the thickness and dielectric constant of the slab, are $0.3a$, $0.55a$, and 12, respectively. Let the radius of the defect holes in the waveguide be $0.44a$, and assume a TE-like wave (the magnetic field mainly parallel to the hole axis) propagates in the PCWs.

When mutually sliding or countersliding two PCWs of the DC along the y direction simultaneously, as shown in the insets of Figs. 3(a) and 3(b), the distances between the second nearest-neighbor coupling defects are always the same. Therefore, $\beta_1 = \beta_2 = \beta$ and Eq. (11) is applied. The shift of the defect holes does not cause symmetry breaking, so the dispersion curves are always crossing in both cases. The blue shift of the dispersion curves is caused by the increase of ω_0 because the effective refractive index of the point defects decreases, in turn increasing the eigenfrequency ω_0 of a point defect when the defect hole moves away from the center of a point defect.

On the other hand, as we simultaneously shift two PCWs of the DC longitudinally along the x direction, as shown in the inset of Fig. 4(a), we would expect that the shift would have not caused the symmetry breaking and therefore their dispersion curves were still crossed since they still possess degenerate dispersions. We found the crossing point shifts

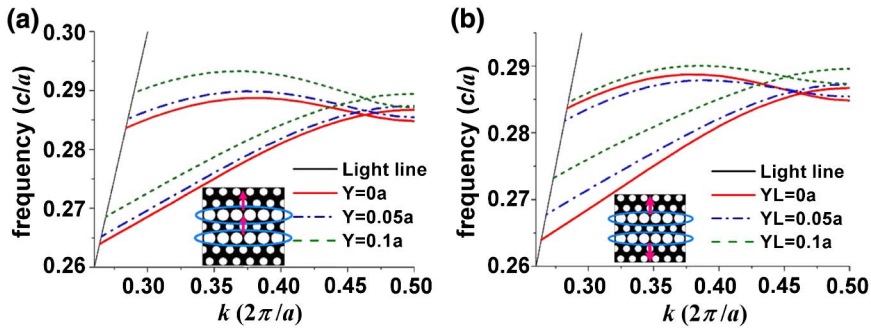

Fig. 3. Dispersion curves of the DCs when (a) mutually sliding and (b) countersliding two waveguides along the y direction. The insets show the cross sections of the simulation structures at $z = 0$.

toward the larger wavenumber as the shifting distance sets to $0.05a$ in Fig. 4(a). This is because $|2\beta/\alpha|$ in Eq. (11) becomes smaller. However, when the shifting distance is $0.1a$, the dispersion curves do not cross anymore because of $|2\beta/\alpha| < 1$, in which the criterion for the crossing dispersion curves fails.

It is even more interesting when one longitudinally countersslides two PCWs, shown in the inset of Fig. 4(b). In this case, the coupling coefficients of the second nearest-neighbor defects become unequal ($\Delta\beta \neq 0$); thus the symmetry of this PCS-DC is broken and Eq. (8) should be applied. The nonzero $\Delta\beta$ removes the degeneracy at all operation frequencies and leads to the fact that the dispersion curves no longer cross. The phase difference of amplitudes in two PCWs has frequency dependence even with a small shift distance as in Fig. 4(b). Such a device has a unique application as a 50/50 beam splitter with a desired phase difference between two outputs and a phase selector to select a designable relative phase between two inputs of the DC for obtaining a maximal output. The design concept is shown as the following.

As an operating frequency is chosen, the electric field amplitudes at the distance $x = na$ in PCW_1 and PCW_2 can be expressed in terms of two eigenmodes with propagation constants k_1 and k_2 as

$$U(x) = Ae^{ik_1x} + Be^{ik_2x}; \tag{12}$$

$$V(x) = Ae^{ik_1x+i\phi_1} - Be^{ik_2x+i\phi_2}, \tag{13}$$

where A and B are the amplitudes contributed from two eigenmodes and ϕ_1 and ϕ_2 are their corresponding phase shifts of PCW_2 relative to PCW_1. When the electric field is incident from PCW_1, which mean $V(0) = 0$, Eqs. (12) and (13) become

$$U(x) = Ae^{ik_1x} + Ae^{ik_2x+i(\phi_1-\phi_2)}; \tag{14}$$

$$V(x) = Ae^{ik_1x+i\phi_1} - Ae^{ik_2x+i\phi_1}. \tag{15}$$

For coupling half of the intensity of the EM wave from PCW_1 into PCW_2, one has $\Delta k\, x = (k_2 - k_1)x = \pi/2$. Thus, the phase difference between two output channels becomes

$$\psi = -i \ln\left\{\frac{1 + Exp[i(\pi/2 + \phi_1 - \phi_2)]}{e^{i\phi_1}(1 + e^{-i\pi/2})}\right\}. \tag{16}$$

It is obvious that the phase difference between the two output channels of a 50/50 splitter made of a PCS-DC can be different from $\pi/2$. The phase shift between two PCWs is mainly dominated by ϕ_1, which can be tuned by the longitudinal countersliding distance between two PCWs; meanwhile, in a conventional beam splitter, $\phi_1 = \phi_2 = 0$, and so the phase difference between the two output channels is always equal to $\pi/2$.

The PCS-DC can also be designed as a phase-selecting device, which can be used in coherent optical communication with optical differential phase-shift keying [24] when there is only a single eigenmode existing in the frequency range, e.g., 0.265–0.282 c/a in Fig. 4(b). Assume the single eigenmode has a propagation constant k; we have the amplitudes of two PCWs $U(x) = Ae^{ikx}$ and $V(x) = Ae^{ikx+i\phi_d}$ with $A = 1$ and $B = 0$, from Eqs. (12) and (13), and a relative phase shift $\phi_d(k)$ determined by Eq. (10). As we inject a local oscillator at the operation frequency to PCW_1 and a data signal having a phase shift of ϕ_s relative to the local oscillator to PCW_2, a maximal output occurs as $\phi_s = \phi_d$; i.e., the phase difference of the data signal relative to the local oscillator equals the phase difference between two PCWs in the eigenmode.

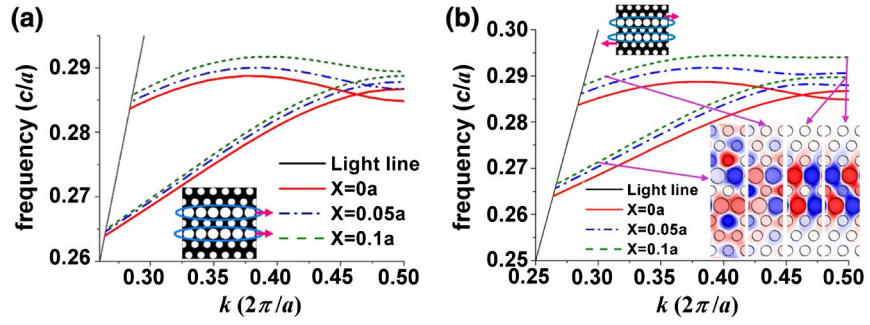

Fig. 4. Dispersion curves of the DCs when (a) mutually sliding and (b) countersliding two waveguides along the x direction. The inset in (a) shows the cross sections of the simulation structures at $z = 0$. The insets in (b) show the eigenmode patterns H_z of the DC with shifting distance $0.1a$ at $k = 0.3$ and 0.5 $(2\pi/a)$ and the simulation structure at the cross section of $z = 0$.

The output intensity at each of PCW outputs equals $[1+\cos(\phi_d-\phi_s)]^2/4$. Therefore, the phase selector can be set for extracting a chosen phase around $\phi_d(k)$. In addition, one can easily control the relative phase ϕ_d of two PCWs through shifting the dispersion curves of the DC toward high or low frequencies using the optical Kerr or electro-optic effect if a nonlinear medium is embedded in the defects of the PCS-DC. Under such a circumstance, the range of the selected phase can be tuned accordingly.

Similarly, our theory can be applied to the 2D cases in which the height of the slab is supposed to be infinite. These equations can also be used to describe the coupling and symmetry-breaking phenomena of two 1D [25] or 2D [26] coupled-resonator optical waveguides [27] when they are close enough.

4. CONCLUSION

We have successfully used the TBT to describe the symmetry breaking in the photonic DC with a triangular lattice. From the derived equations, we found the dispersion curves will cross only when the second nearest-neighbor coupling coefficients between two waveguides are the same ($\beta_1=\beta_2=\beta$). Otherwise, the dispersion curves will be anticrossing; i.e., the dispersion curves do not cross. For example, when mutually sliding or countersliding two PCWs of a DC perpendicular to the propagation direction, the two next nearest-neighbor coupling coefficients are always equal to each other. The symmetry that results in crossing of dispersion curves does not break and the decoupling point always exists. When mutually sliding along the propagation direction, symmetry breaking is not observed, but the crossing point moves toward a high wavevector due to the smaller ratio between the next nearest-neighbor and nearest-neighbor coupling coefficients, i.e., a decrease of $|2\beta/\alpha|$. The crossing point disappears when the sliding distance increases. This is because the criterion for the crossing of dispersion curves fails.

Longitudinally countersliding two PCWs by the same distance makes nonequal next nearest-neighbor couplings, i.e., $\beta_1\neq\beta_2$, which causes the symmetry breaking. Under this circumstance, the dispersion curves split and are anticrossing. There exists a phase shift between the two PCWs. Such a symmetry-breaking DC can be used as a 50/50 beam splitter or a phase selector, in which the output phase can be tuned by varying either the countersliding distance or the refractive index of the defects of the two PCWs.

ACKNOWLEDGMENTS

The authors acknowledge partial financial support from the X-Photonics Interdisciplinary Center of National Chiao Tung University and the National Science Council of the Republic of China under grants NSC99-2112-M009-009-MY3 and NSC99-2221-E009-095-MY3.

REFERENCES

1. L. Liu, M. H. Pu, K. Yvind, and J. M. Hvam, "High-efficiency large-bandwidth silicon-on-insulator grating coupler based on a fully-etched photonic crystal structure," Appl. Phys. Lett. **96**, 051126 (2010).
2. B. Momeni, S. Yegnanarayanan, M. Soltani, A. A. Eftekhar, and E. S. Hossieni, "Silicon nanophotonic devices for integrated sensing," J. Nanophoton. **3**, 031001 (2009).
3. S. W. Ha, A. A. Sukhorukov, K. B. Dossou, L. C. Botten, A. V. Lavrinenko, D. N. Chigrin, and Y. S. Kivshar, "Dispersionless tunneling of slow light in antisymmetric photonic crystal couplers," Opt. Express **16**, 1104–1114 (2008).
4. T. B. Yu, M. H. Wang, X. Q. Jiang, Q. H. Liao, and J. Y. Yang, "Ultracompact and wideband power splitter based on triple photonic crystal waveguides directional coupler," J. Opt. A **9**, 37–42 (2007).
5. L. Petti, M. Rippa, J. Zhou, L. Manna, and P. Mormile, "A novel hybrid organic/inorganic photonic crystal slab showing a resonance action at the band edge," Nanotechnology **22**, 285307 (2011).
6. K. Asakawa, Y. Sugimoto, Y. Watanabe, N. Ozaki, A. Mizutani, Y. Takata, Y. Kitagawa, H. Ishikawa, N. Ikeda, K. Awazu, X. Wang, A. Watanabe, S. Nakamura, S. Ohkouchi, K. Inoue, M. Kristensen, O. Sigmund, P. I. Borel, and R. Baets, "Photonic crystal and quantum dot technologies for all-optical switch and logic device," New J. Phys. **8**, 208 (2006).
7. V. R. Almeida, C. A. Barrios, R. R. Panepucci, and M. Lipson, "All-optical control of light on a silicon chip," Nature **431**, 1081–1084 (2004).
8. G. Calo, A. D'Orazio, M. Grande, V. Marrocco, and V. Petruzzeli, "Active InGaAsP/InP photonic bandgap waveguides for wavelength-selective switching," IEEE J. Quantum Electron. **47**, 172–181 (2011).
9. K. Suzuki and T. Baba, "Nonlinear light propagation in chalcogenide photonic crystal slow light waveguides," Opt. Express **18**, 26675–26685 (2010).
10. A. Mekis, J. C. Chen, I. Kurland, S. H. Fan, P. R. Villeneuve, and J. D. Joannopoulos, "High transmission through sharp bends in photonic crystal waveguides," Phys. Rev. Lett. **77**, 3787–3790 (1996).
11. A. Sharkawy, S. Y. Shi, D. W. Prather, and R. A. Soef, "Electro-optical switching using coupled photonic crystal waveguides," Opt. Express **10**, 1048–1059 (2002).
12. D. W. Prather, S. Shi, J. Murakowski, G. J. Schneider, A. Sharkawy, C. Chen, and B. Miao, "Photonic crystal structures and applications: perspective, overview, and development," IEEE J. Sel. Top. Quantum Electron. **12**, 1416–1437 (2006).
13. E. Bulgakov and A. Sadreev, "Switching through symmetry breaking for transmission in a T-shaped photonic waveguide coupled with two identical nonlinear micro-cavities," J. Phys. Condens. Matter **23**, 315303 (2011).
14. B. Maes, B. M. Soljacic, J. D. Joannopoulos, P. Bienstman, R. Baets, S. P. Gorza, and M. Haelterman, "Switching through symmetry breaking in coupled nonlinear micro-cavities," Opt. Express **14**, 10678–10683 (2006).
15. M. Bayindir, B. Temelkuran, and E. Ozbay, "Photonic-crystal-based beam splitters," Appl. Phys. Lett. **77**, 3902 (2000).
16. I. Abdulhalim, "Reflective phase-only modulation using one-dimensional photonic crystals," J. Opt. A **2**, L9–L11 (2000).
17. C. H. Huang, W. F. Hsieh, and S. C. Cheng, "Tuning the decoupling point of a photonic-crystal directional coupler," J. Opt. Soc. Am. B **26**, 203–209 (2009).
18. F. S. S. Chien, J. B. Tu, W. F. Hsieh, and S. C. Cheng, "Tight-binding theory for coupled photonic crystal waveguides," Phys. Rev. B **75**, 125113 (2007).
19. F. S. S. Chien, Y. J. Hsu, W. F. Hsieh, and S. C. Cheng, "Dual wavelength demultiplexing by coupling and decoupling of photonic crystal waveguides," Opt. Express **12**, 1119–1125 (2004).
20. S. G. Johnson and J. D. Joannopoulos, "Block-iterative frequency-domain methods for Maxwell's equations in a planewave basis," Opt. Express **8**, 173–190 (2001).
21. D. N. Christodoulides and N. K. Efremidis, "Discrete temporal solitons along a chain of nonlinear coupled microcavities embedded in photonic crystals," Opt. Lett. **27**, 568–570 (2002).
22. C. H. Huang, J. N. Wu, P. Y. Lee, W. F. Hsieh, and S. C. Cheng, "The properties and design concepts of photonic directional couplers made of crystal slabs," J. Phys. D **43**, 465103 (2010).
23. J. D. Joannopoulos, S. G. Johnson, J. N. Winn, and R. D. Meade, *Photonic Crystals: Modeling the Flow of Light* (Princeton University, 2008).

24. G. Li, "Recent advances in coherent optical communication," Adv. Opt. Photon. **1**, 279–307 (2009).
25. Q. M. Quan, P. B. Deotare, and M. Loncar, "Photonic crystal nanobeam cavity strongly coupled to the feeding waveguide," Appl. Phys. Lett. **96**, 203102 (2010).
26. S. Mookherjea and A. Yariv, "Coupled resonator optical waveguides," IEEE J. Sel. Top. Quantum Electron. **8**, 448–456 (2002).
27. A. Yariv, Y. Xu, R. K. Lee, and A. Scherer, "Coupled-resonator optical waveguide: a proposal and analysis," Opt. Lett. **24**, 711–713 (1999).